Preprint PFC/JA-84-8

SPECTRAL MEASUREMENTS FROM A TUNABLE, RAMAN, FREE ELECTRON MASER

J. Fajans, G. Bekefi, Y.Z. Yin, and B. Lax

Plasma Fusion Center and
Research Laboratory of Electronics
Massachusetts Institute of Technology
Cambridge, MA. 02139

March 1984

Spectral Measurements from a Tunable, Raman, Free Electron Maser

J. Fajans, G. Bekefi, Y.Z. Yin[†], and B. Lax
Department of Physics and Research Laboratory of Electronics
Massachusetts Institute of Technology
Cambridge, MA 02139

Abstract

We report narrow band spectra ($\Delta\omega/\omega \leq 0.02$) from a tunable ($7 \leq \omega/2\pi \leq 18$GHz), Raman free electron maser operating in a single TE_{11} waveguide mode. RF power levels of 20kW and efficiencies of $\sim 5\%$ have been achieved. Measured dispersion characteristics are in good agreement with theory.

[†]Permanent address: Institute of Electronics, Academia Sinica, Beijing, People's Republic of China.

One of the outstanding properties of free electron lasers[1,2,3] (FEL), or masers, is their inherent tunability. Frequency tuning of coherent, narrow-band radiation can be achieved, at least in principle, by changing the accelerator voltage. In this paper we present what we believe is the first detailed study of the frequency versus voltage tuning of both the high and the low frequency branches of the FEL instability under high current-density (Raman) operation. Since scanning the beam velocity is equivalent to scanning the phase velocity of the ponderomotive[2] bunching force, our study thus addresses the physics of the wave dispersion characteristics.

The experimental arrangement is illustrated in Fig. 1a. A thermionically emitting Pierce gun (250kV, 250A) from a SLAC klystron (model 343) is energized by the Physics International Pulserad 615MR high voltage facility (500kV, 4kA, 15μs). The ensuing converging electron beam is guided by an assembly of magnetic focusing coils into a 2.54cm ID stainless steel, evacuated drift tube which also acts as the cylindrical microwave waveguide. The maximum beam current density is 40Acm^{-2}. Beam integrity is maintained by a uniform axial guide magnetic field $B_{||}$ ranging from 0.7 to 7kG. Computer simulations indicate the the beam is of good quality with an energy spread of less that 1%. The 50 period circularly polarized magnetic wiggler has a period $l = 3.3$cm, an amplitude of $B_w = 1.5$kG (maximum), and is generated by means of bifilar conductors wound on the drift tube. An aperture placed before the wiggler (see Fig. 1a) limits the beam radius r_b to 0.25cm, so that the product $k_w r_b$ ($k_w = 2\pi/l$) is less than 0.5. This ensures[3,4,5] that the electrons are subjected to an essentially pure circularly polarized wiggler field. The first six periods of the wiggler are resistively loaded[6] to produce a smooth increase in the magnetic field amplitude at the wiggler entrance. Together with the limited beam radius, this adiabatic entrance assures high quality electron orbits. The entire magnetic system (gun coils, solenoid, and wiggler) is energized by capacitor banks whose half periods (0.25 and 40ms) are long compared with the electron beam pulse (15μs), thereby generating magnetic fields that are essentially quasi-static.

The circularly polarized radiation propagating in the cylindrical drift tube has

a duration of several microseconds. A TE_{11} circular guide to TE_{10} rectangular guide transformer couples half of the FEL emission out of the system in the form of a linearly polarized wave traveling in a rectangular guide. Power levels are determined by means of a calibrated crystal detector. Up to 20kW of microwave radiation and efficiencies of up to 5% in converting electron beam power to microwave power have been observed. The saturated efficiency estimated from theory[2] is $\sim 4\%$. There is no measurable radiation when the wiggler magnetic field is turned off. Fig. 2 illustrates the sharp onset of emission at a threshold wiggler field amplitude of 128G.

To measure[7] the spectral characteristics of the emission, the radiation first impinges on a microwave switch which allows passage of a 40ns burst into a 150m long X-band waveguide dispersive line. The output from the dispersive line, together with the undispersed signal, are displayed on a fast oscilloscope, as illustrated in Fig. 1b. The spectral width of the emission is less than 2%. Occasionally, two, rather than just one line are observed (Fig. 1c). We show below that the two modes correspond to the low and high frequency branches of the free electron maser instability.

The emission from a Raman free electron maser results from the interaction between the slow space-charge wave on the electron beam

$$\omega = \beta_{\|} c(k + k_w) - p_1 \omega_p / \gamma^{3/2} \tag{1}$$

and the electromagnetic waveguide mode

$$\omega^2 = c^2 k^2 + (w_c^2 + p_2^2 w_p^2 / \gamma) \tag{2}$$

Here ω and k are the radiation frequency and wave number, respectively; ω_c is the relevant waveguide cutoff frequency; $\beta_{\|} = v_{\|}/c$ with $v_{\|}$ as the axial beam velocity; $\gamma = (1 - \beta_{\|}^2 - \beta_{\perp}^2)^{-1/2}$; $\beta_{\perp} = v_{\perp}/c$ is the transverse velocity acquired by the electrons from the the wiggler magnetic field; $\omega_p = (Ne^2/m_0\epsilon_0)^{1/2}$ is the nonrelativistic plasma frequency; and p_1 and p_2 are numerical factors[8] less than unity which take account of the finite transverse geometry of the experiment. Solving Eqs. (1) and (2) in the $\omega_p \to 0$ limit, which is appropriate to our experimental

conditions, leads to the radiation frequency

$$\omega = \beta_{\|} c k_w \gamma_{\|}^2 \left\{ 1 \pm \beta_{\|} \left[1 - \left(w_c / k_w \gamma_{\|} \beta_{\|} c \right)^2 \right]^{1/2} \right\} \tag{3}$$

where $\gamma_{\|} = (1 - \beta_{\|}^2)^{-1/2}$ and where $\pm$ represents the high and low frequency branches of the FEL instability, respectively. In our experiment, $k_w \beta_{\|} c < \omega_c$, and thus both waves propagate in the direction of the electron beam.

The solid and dashed lines illustrated in Figs 3a and b are the radiation frequencies as a function of beam voltage V calculated from Eq. (3) using the parameters appropriate to our experiment (ω_c is the cutoff frequency of the TE_{11} fundamental mode of the circular waveguide). We see that as V decreases, the high and low frequency branches approach one another; they merge into a single radiating mode when the beam velocity $v_{\|}$ equals the group velocity of the electromagnetic wave of Eq. (2). We note from Fig. 3 that for a given voltage V, the frequency decreases with increasing wiggler amplitude B_w because, as B_w goes up, the perpendicular velocity $v_{\perp}$ increases in conformity with the equation[4,5]

$$\beta_{\perp} = |\Omega_w \beta_{\|} / \left[\gamma k_w \beta_{\|} c - \Omega_{\|} \right]^{-1}| \qquad (\gamma k_w \beta_{\|} c \neq \Omega_{\|}) \tag{4}$$

which leads to a reduction in $\beta_{\|}$ and $\gamma_{\|}$ of Eq. (3). (Here $\Omega_w = eB_w/m_0$ and $\Omega_{\|} = eB_{\|}/m_0$ are the nonrelativistic cyclotron frequencies in the wiggler and guide magnetic fields, respectively).

The triangles and solid dots of Fig. 3a represent spectral measurements made with the waveguide dispersive line, as described above. However, the dispersive line has a limited frequency capability (7-12GHz), and, in order to extend the range of our observations, and to improve our measuring accuracy, we adopted the following alternative technique. We reduced the wiggler amplitude to just below its threshold value so that the emitted radiation was less than a milliwatt. We then injected a low level ($\sim$ 100mW) monochromatic CW signal of known frequency $\omega/2\pi$ into the wiggler region from the direction of the microwave window (Fig. 1a), thereby "stimulating" the emission process. The stimulated signal was then observed by means of a crystal detector. Figure 4 illustrates a

typical shot. Since the accelerator has an RC droop, the beam energy sweeps through a range of values as seen in Fig. 4a. Stimulation occurs (Fig. 4b) at a time during the voltage pulse when the voltage reaches its appropriate value. Varying the injected frequency on successive shots allows one to trace the frequency-voltage characteristics of the FEL instability. The experimental results are shown in Fig. 3b.

The measurements described hitherto were carried out at a low guide magnetic field $B_{\|} = 1620G$, below the resonant field defined as (see Eq. (4)) $\Omega_{\|}(\text{resonant}) = \gamma k_w \beta_{\|} c$. Experiments (not shown) performed well above resonance ($B_{\|} \geq 4000\text{G}$) show that the emission frequency far from resonance is virtually independent of $B_{\|}$, in agreement with Eq.(3). This demonstrates that the cyclotron maser (gyrotron) instability has not been excited, which is always a worrisome possibility.[9] The interesting region around resonance has not yet been studied by us.

In conclusion, we have described the operation of a narrow band ($\Delta\omega/\omega < 0.02$) free electron maser that can be continuously tuned in frequency by more than a factor of two. The emission occurs in a single (TE_{11}) waveguide mode. The voltage versus frequency characteristics are in good agreement with theory. It is noteworthy that our device operates efficiently at low guide magnetic fields (below resonance). This has important implications when one wishes to scale to higher frequencies corresponding to millimeter and submillimeter wavelengths. Had the required $B_{\|}$ been above resonance, prohibitively large guide fields would become necessary.

Aknowledgements

This work was supported in part by the National Science Foundation and in part by the Hertz Foundation.

References

[1] J. A. Edighoffer, G. R. Neil, C. E. Hess, T. I. Smith, S. W. Fornaca, and H. A. Schwettman, *Phys. Rev. Lett.* **52**, 344 (1984), and references therein.

[2] P. Sprangle, R. A. Smith, and V. L. Granatstein, *Infrared and Millimeter*

Waves, K. J. Button, eds. Vol. 1, Academic Press, N.Y., 279 (1979), and references therein. Also R. M. Phillips, *IRE Trans. Elect. Dev.* **ED-7**, 231 (1960).

[3] S. H. Gold, W. M. Black, H. P. Freund, V. L. Granatstein, R. H. Jackson, and P. C. Efthimion, A. K. Kincaid, *Phys. Fluids.* **26**, 2683 (1983).

[4] L. Friedland, *Phys. Fluids.* **23**, 2376 (1980).

[5] H. P. Freund, and A. T. Drobot, *Phys. Fluids.* **25**, 736 (1982).

[6] J. Fajans,, *J. Appl. Phys.* **55**, 43 (1984).

[7] T. J. Orzechowski, and G. Bekefi, *Phys. Fluids.* **22**, 978 (1979).

[8] G. M. Branch, and T. G. Mihran, *IRE Trans. Elect. Dev.* **ED-2**, 3 (1955).

[9] R. E. Shefer and G. Bekefi, *Int. J. Electronics.* **51**, 569 (1981).

Figure Captions

Figure. 1 (a) Experimental arrangement. (b) Dispersive line data showing the undispersed signal (left) and the high frequency dispersed mode (I) right; (c) data showing both the high frequency mode (I) and the low frequency mode (II).

Figure. 2 Total microwave power as a function of B_w ($B_{||} = 1620$G).

Figure. 3 Radiation frequency as a function of beam voltage V as measured with (a) dispersive line; (b) near B_w(threshold) by injection of a stimulating signal (see text) ($B_{||} = 1620$G). Experimental error in measured quantities $\leq 2\%$.

Figure. 4 (a) Time history of the beam voltage V; (b) trace 1 is the amplitude of a 10.4GHz injected CW signal; trace 2 is the stimulated FEL signal (see text).

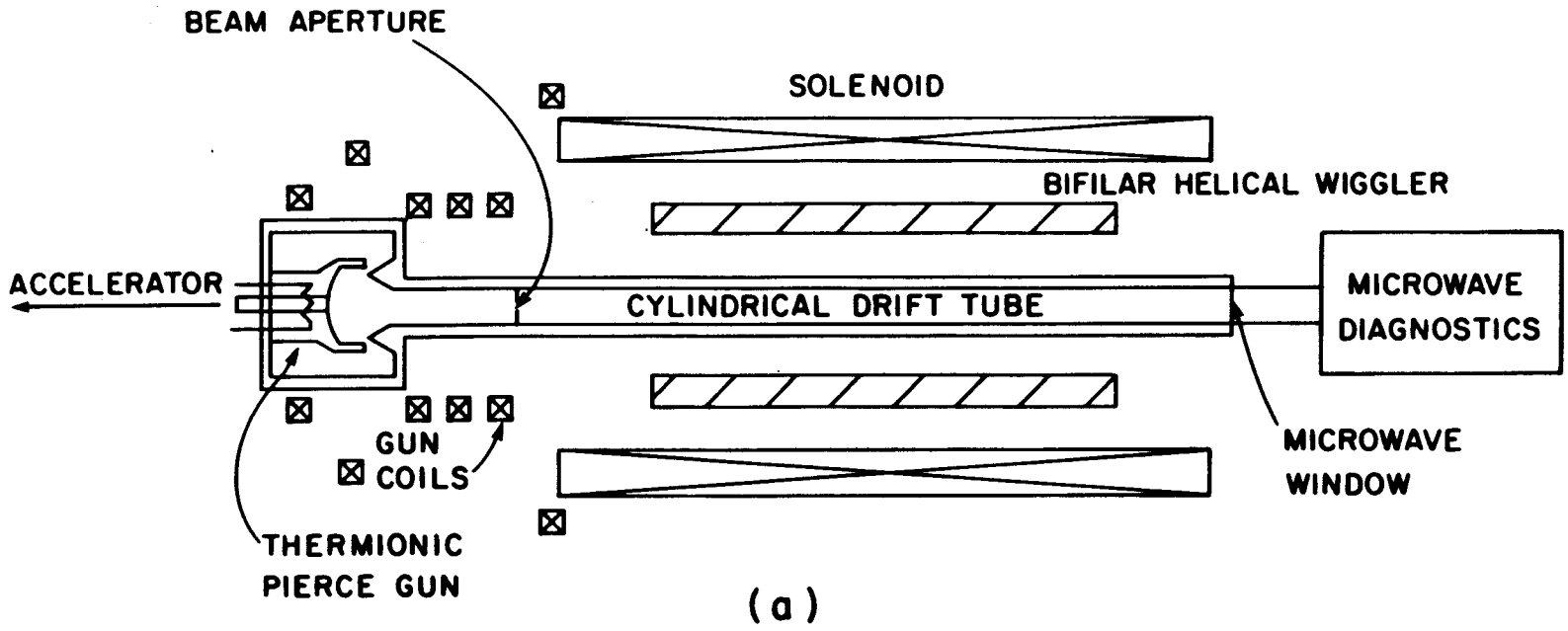

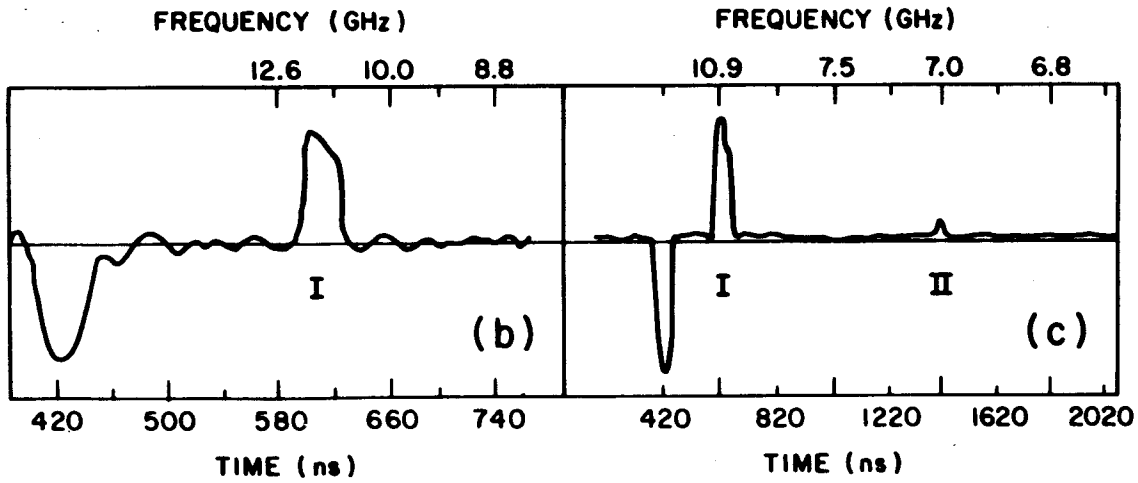

Fig. 1
Fajans, Bekefi, Yin, Lax

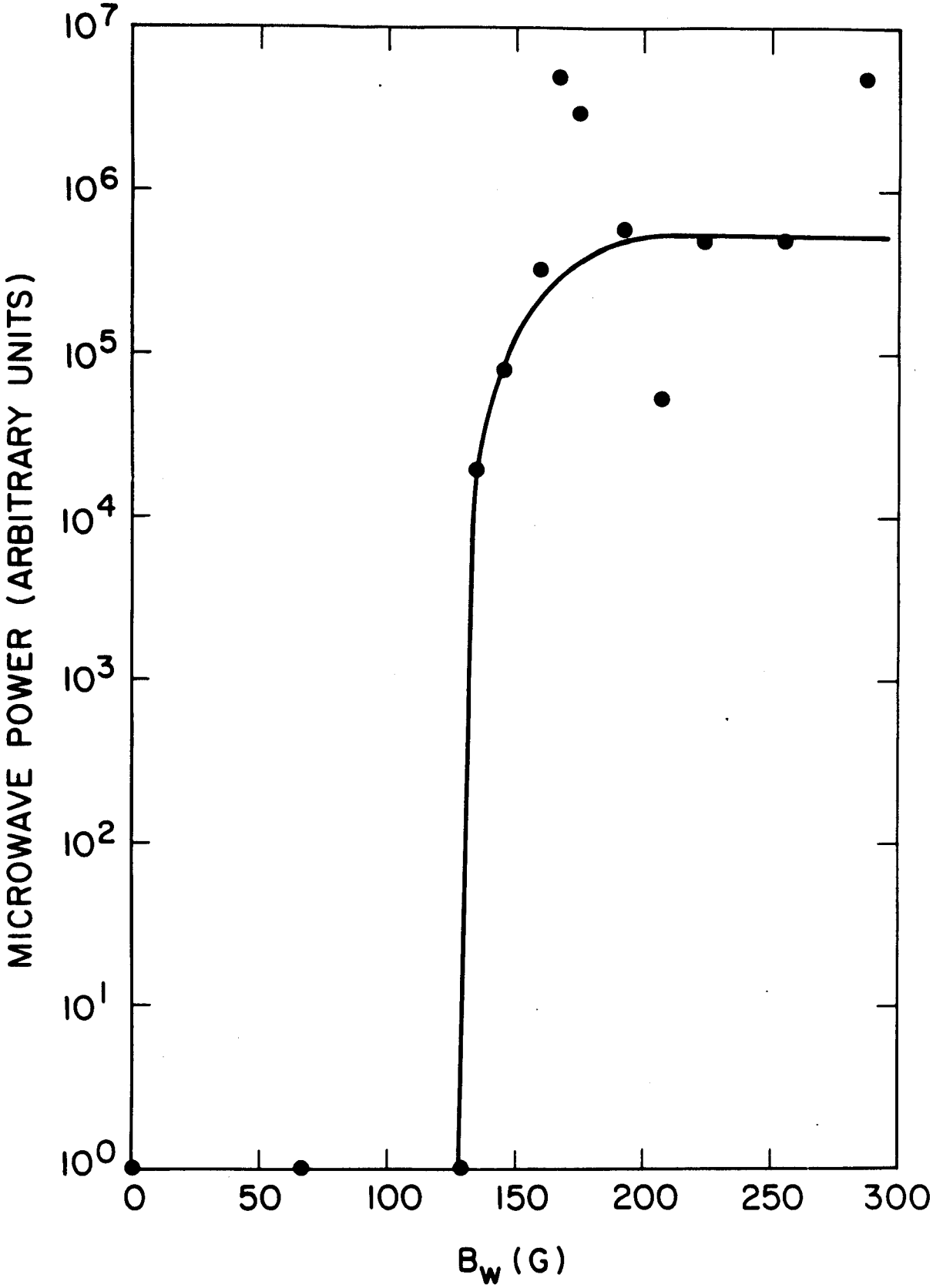

Fig. 2
Fajans, Bekefi, Yin, Lax

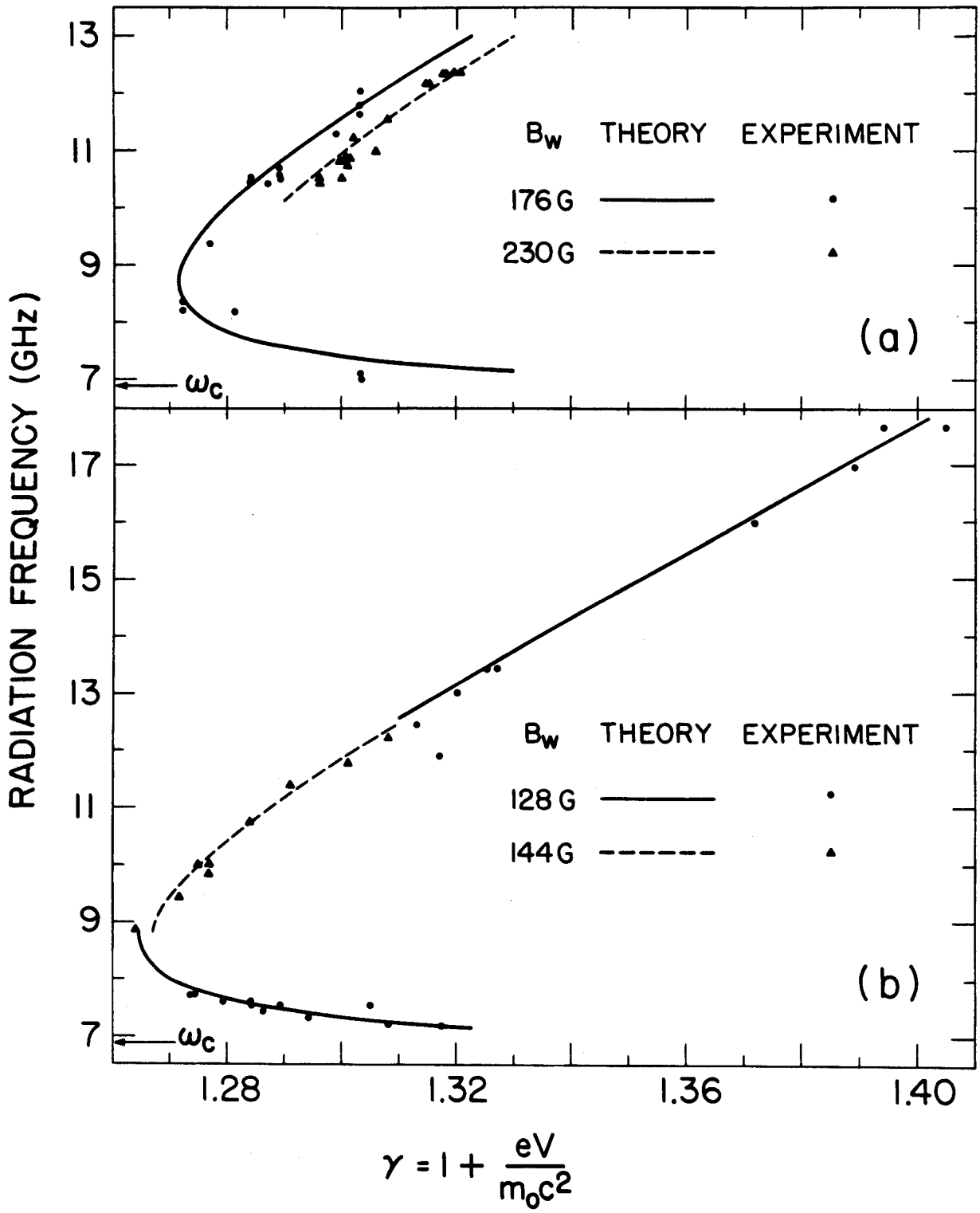

Fig. 3
Fajans, Bekefi, Yin, Lax

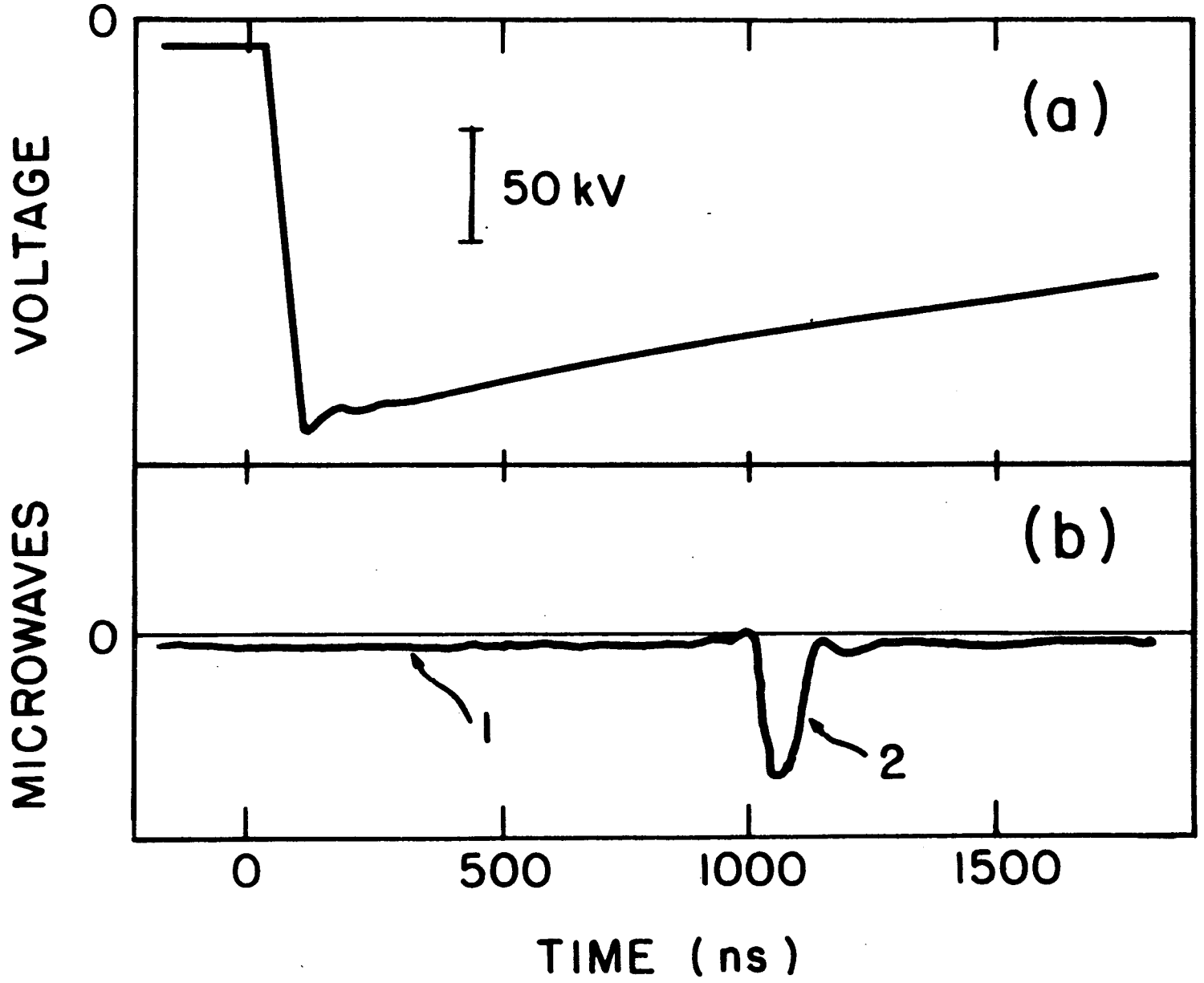

Fig. 4
Fajans, Bekefi, Yin Lax